A systematic analysis of the joint effects of ganglion cells, lagged LGN cells, and intercortical inhibition on spatiotemporal processing and direction selectivity

René Larisch [1,*], and Fred H. Hamker [1,**]

January 29, 2024

[1] *TU Chemnitz, Dept. of Computer Science, Artificial Intelligence*

[*] *rene.larisch@informatik.tu-chemnitz.de*

[**] *fred.hamker@informatik.tu-chemnitz.de*

Simple cells in the visual cortex process spatial as well as temporal information of the visual stream and enable the perception of motion information. Previous work suggests that the direction selectivity of V1 simple cells is associated with a temporal offset in the thalamocortical input stream through lagged and non-lagged cells of the lateral geniculate nucleus (LGN), but also with intercortical inhibition. While there exists a large corpus of models for spatiotemporal receptive fields, the majority of them built-in the spatiotemporal dynamics by utilizing a combination of spatial and temporal functions and thus, do not explain the emergence of spatiotemporal dynamics on basis of network dynamics emerging in the retina and the LGN. In order to better comprehend the emergence of spatiotemporal processing and direction selectivity, we used a spiking neural network to implement the visual pathway from the retina to the primary visual cortex. By varying different functional parts in our network, we demonstrate how the direction selectivity of simple cells emerges through the interplay between two components: tuned intercortical inhibition and a temporal offset in the feedforward path through lagged LGN cells. Further, we observe that direction-selective simple cells are linked to a particular spiking pattern in a local excitatory-inhibitory circuit: If

the stimulus moves in the non-preferred direction of a simple cell, inhibitory neurons with a different spatial position or tuning spike earlier, preventing the simple cell to spike. However, in the preferred direction, these inhibitory cells spike later, enabling the simple cell to spike.

Author summary

The origin of spatiotemporal receptive fields of layer 4 simple cells, and their selectivity for a certain moving direction of a stimulus has been investigated in a large corpus of model studies. The majority of these studies utilize a functional description to approximate the behavior of the previous areas along the visual pathway. Therefore, the emergence of spatiotemporal processing as a consequence of local neuronal dynamics in the preceding layers is not well understood. Here, we systematically analyze the different functional parts of a spiking neural network, resembling the early visual pathway, starting with retinal ganglion cells up to simple and inhibitory cells in layer 4. Our simulations show, how an initial spatiotemporal processing emerges by a delay in the ganglion surrounding field. Our work highlights the combined effect of tuned intercortical inhibition and lagged LGN cells for the direction selectivity of simple cells. While inhibition alone leads to a sharp orientation tuning, but to a bidirectional selectivity, lagged LGN cells implement a temporal offset in the thalamocortical input currents, giving one moving direction a temporal advantage, leading to an unidirectional selectivity.

1 Introduction

Simple cells in the primary visual cortex (V1) are selective for a wide range of features like orientation, spatial frequency [1, 2, 3, 4], or stimulus movement direction [1, 5, 6, 7]. Models of object recognition mainly rely on the spatial receptive field properties (like orientation selectivity). However, it has been shown that the ON- and OFF-fields of a simple cell receptive field are not static, but change on a millisecond time scale, indicating a spatiotemporal behavior, described as a spatiotemporal receptive field (STRF) [8, 9]. Depending on how the spatial profile of the receptive field changes over time, a STRF can be classified as a separable or inseparable one [10]. A separable STRF can be mathematically modeled by two separable functions, one for the space domain to describe the spatial selectivity of the cell, and one for the time domain to describe the change of the neuron response profile over time as a switch in the polarity of the spatial receptive field [9]. In contrast, an inseparable STRF shows a transition in space over time [10, 11, 12, 13]. Besides simple cells with an STRF can be assigned as separable or inseparable, a continuum between these two types of STRFs has been observed [10].

A spatiotemporal behavior has also been reported for thalamocortical cells in the lateral geniculate nucleus (LGN), in particular, their center-surround antagonism receptive field reverses its polarity over time

[9, 13, 14]. It has been discussed previously, that a temporal offset between cells in the LGN, those that respond immediately to a stimulus and cells that react with a delay of several milliseconds (so-called lagged LGN cells) may cause inseparable STRFs of V1 simple cells [15]. Further, McLean et al. [11] reported that simple cells with an inseparable STRFs are direction selective, while most cells with a separable STRF are not. Due to this, it has bee assumed that both, inseparable STRFs and direction selectivity are caused by the temporal offset in the LGN [15, 11, 9], linking the simple cell direction selectivity with the inseparability of the corresponding STRF. This assumption has been supported by several model studies, demonstrating how the combined input of non-lagged and lagged cells can lead to the emergence of inseparable STRFs [16, 17, 18], and that simple cells with an inseparable STRF are more tuned for a particular direction than cells with a separable STRF [16, 19, 18].

Studies with mice [20, 21], cats [5, 6] and ferrets [7] suggest a role of intercortical inhibition on the origin of direction selectivity. Priebe and Ferster [5] showed in a study of cat primary visual cortex that the excitatory and inhibitory input currents are tuned for the same direction, but are evoked asynchronously in time. Li et al. [21] reported in a study of the mice visual cortex that excitatory synaptic input arrives earlier than inhibitory synaptic input at the preferred direction of the corresponding cell to drive the cell to spike, while at the opposite direction, inhibition arrives earlier. This led to several model studies, which assume that direction selectivity is caused either alone by intercortical inhibition [22, 23], or by the combination of a temporal offset from LGN (as caused by lagged LGN cells) and intercortical inhibition [18, 24, 25, 26]. It has been suggested that the lagged and non-lagged LGN cells create a temporal offset in the input stream, leading to an initial direction selectivity, which is increased through lateral inhibition by suppressing the activity in the null direction [24, 26].

While these model studies are successful in modeling simple cell spatiotemporal receptive fields and direction selectivity, the temporal dynamics of LGN or simple cells is mainly implemented with a temporal function and not incorporating explicit local neuronal dynamics [17, 18, 16, 24, 25, 26] prohibiting to understand how simple cell STRFs can emerge by the local neuronal dynamics along the visual pathway. To improve our understanding of the emergence of STRFs, the role of lagged LGN cells, and intercortical inhibition for direction selectivity, we present a systematic analysis in a spiking neural network, modeling the visual pathway from the retinal ganglion cells to the primary visual cortex. We assume that a delay in the surround field of the ganglion cells leads to a temporal decoupling of the processing of visual information along the center and the surround, sending a phasic signal to the cortex. The connectivity matrix from the LGN cells to the V1 simple cells and inhibitory interneurons has been obtained by prior training on natural scenes to ensure a realistic connectome in our network. By systematically changing the tuning of intercortical inhibition and the temporal offset caused by non-lagged and lagged LGN cells, we investigate their role in the emergence of direction selectivity. Our results suggest that tuned intercortical

inhibition alone enables a sharp orientation tuning, but shows a symmetric, bidirectional response profile. A temporal offset in the thalamocortical input, as introduced between lagged and non-lagged LGN cells, is necessary to break this symmetry and enable the emergence of unidirectional selectivity. Further, we observe resulting network dynamics, as they have been reported before, such as that pyramidal cells with a high unidirectional selectivity, receive inhibition at the preferred direction later than excitation, while at the non-preferred direction, the excitatory and inhibitory currents arrive at the same time and cancel each other out.

To the best of our knowledge, we present the first spiking neural network utilizing the delay in the RGC surround fields, lagged LGN cells, as well as intercortical inhibition to enable spatiotemporal processing of V1 simple cells. We demonstrate that direction selectivity can emerge through the combination of lagged LGN cells and tuned intercortical inhibition.

2 Methods

The spiking neural network has been implemented in Python 3.8 and by the ANNarchy simulator (v4.7.1) [27]. Source code of the spiking network and evaluations are available at `https://github.com/hamkerlab/Larisch2024_Spatiotemporal_Processing`.

2.1 Network architecture

The model presented here is based on the V1 layer 4 model proposed in our previous work [28], but extended by input processing to enable the emergence of spatiotemporal behavior. Due to this, the network implements three different stages of the visual stream, from the retina via the lateral geniculate nucleus to layer 4 of the primary visual cortex (see **Fig. 1**).

Retina The first stage implemented in the network contains the retinal ganglion cells (RGC). We model the input weights for a RGC with a two-dimensional difference of Gaussian (DoG) function, a common function to model the spatial center-surround organization of the RGC receptive fields [29, 30], where the ON-fields provide excitatory input and the OFF-fields inhibitory input. This mimics the joint effect of the bipolar cells and the inhibitory horizontal cells, and the bipolar cells and inhibitory amacrine cells in the retina [31, 32]. The receptive fields sample from a 5×5 pixel input. With a spacing of 2 pixels between two neighboring cells, the complete population receives a monochrome 48×48 pixel input. The DoG functions of two adjacent cells have an overlap of 3 pixels. The model implements the ON- and OFF-pathway via two populations of RGCs. The ON-pathway consists of ON-centered cells and the OFF-pathway of OFF-centered cells. Thus, the complete RGC layer consists of $22\times22\times2$ cells arranged spatially on a 2D-grid to process the input. The RGCs are modeled with adaptive integrate-and-fire neurons [33], receiving

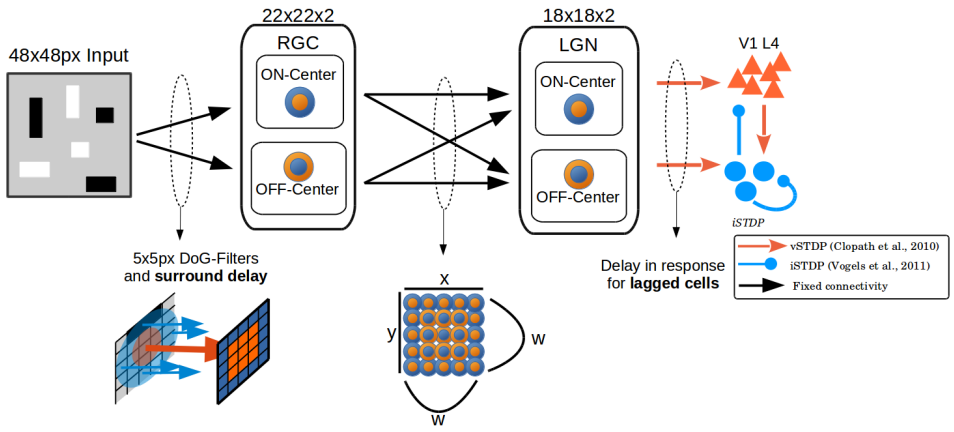

Figure 1: **Network architecture.** A 48×48 pixel input is presented to the input layer and sent to two populations of retinal ganglion cells (RGC). One population consists of ON-center cells and the other of OFF-center cells to mimic the ON- and OFF-path. The input weights of the RGCs are modeled as a Difference of Gaussian so that each RGC receives a 5×5 pixel input. A delay can be added to the weights of the DoG surround field. A LGN cell receives input from a grid of 5×5 RGC to preserve the spatial arrangement. To enable the center-surround antagonism in LGN, an LGN cell receives input from 3×3 ganglion cell grid of the same polarity for the center, and a ring of 16 ganglion cells with the opposite polarity for the surround. The weights from the ganglion to the LGN cell follow a spatial Gaussian distribution, with higher weights in the center and lower weights in the surround field. Both LGN populations are connected to a population of excitatory and inhibitory cells, whose connections are learned on natural scenes. A lag in the transfer of an LGN spike can be added to implement lagged LGN cells.

a continuous excitatory (via the ON-field) or inhibitory (via the OFF-field) input current.

We add a delay to surround fields of the RGCs, as reported, e.g. for bipolar cells in the retina of mammalian [34] and non-mammalian species [35, 36].Its value was drawn from a discrete uniform distribution between 30 ms and 50 ms, relative to the center weights.

Lateral geniculate nucleus The LGN layer consists of two LGN populations, implementing the ON- and OFF-pathway, each with 18×18 LGN cells, arranged on a 2D grid. To realize the center-surround antagonism, each LGN cell receives input from the RGC population with the same polarity for the center field and from RGC cells with an opposite polarity for the surround field, similar as it is reported for retinogeniculate connections in cats [14]. For example, an ON-center with OFF-surround LGN cell is connected to 9 (in a 3×3 grid) RGCs in the ON-population and to 16 (to assemble the surround field) cells in the OFF-population (and vice versa for an OFF-centered, ON-surround LGN cell).

As studies reported that some LGN cells respond with a delay of 30 ms to 70 ms to the stimulus onset (so-called lagged LGN cells) [15, 37, 38], we implemented a synaptic delay on the outgoing synapses of a subgroup of LGN neurons to create a lag in the transmission of the LGN spikes, accounting for observed lagged LGN cells.

Layer 4 of primary visual cortex Both LGN populations (ON- and OFF-center) project to a population of excitatory and inhibitory neurons resembling layer 4 of the primary visual cortex (V1). The excitatory population consists of 324 neurons and the inhibitory one of 81 neurons to match the 4:1 ratio, as reported for different species as in the striate cortex of cats [39], monkeys [40] and in rodents [41]. Inhibitory neurons receive additional input from the excitatory neurons, sending inhibitory input back to the excitatory neurons, and they are connected to other inhibitory neurons of their population (no self-inhibition). To ensure the emergence of Gabor-like receptive fields in the excitatory and inhibitory population, and of a structured connectivity between these two populations we pre-trained the weights to and between both populations in a separate training step. In this training step, 400,000 randomly chosen patches of natural scenes [42] are presented. The learning of these connections was done separately, without the RGC population, and with a Poisson neuron model in the LGN. A detailed description of the training and properties of the resulting network can be found in Larisch et al. [28]. After that, no further learning took place and every other connection in this network is fixed. As the synapses of the network were initialized randomly for the pre-training, we trained 5 different network instances to ensure, that the observed dynamics were not caused by random effects through the initialized synapses. Each network instance represents one complete model with a different set of pre-trained weights. We performed all analyses on each of the five network instances.

2.1.1 Neuron model

All neurons in the RGC and LGN are implemented on the basis of the adaptive exponential integrate-and-fire neuron model (AdEx) as described in Brette and Gerstner [33]. The membrane potential (V) develops as described in Eq.1 and depends on the input I, representing the sum over the excitatory and inhibitory input current into the neuron, and the adaptive current w (see Eq.2). If V exceeds the spiking threshold (V_T) the exponential term increases promptly resulting in a rapid increase of the membrane potential. After each spike, w is increased by a value b, and V is set to V_r.

$$C\frac{dV}{dt} = -g_L(V - E_L) + g_L\Delta_T e^{\frac{V-V_T}{\Delta_T}} - w_{ad} + I \tag{1}$$

$$\tau_{w_{ad}}\frac{dw_{ad}}{dt} = a(V - E_L) - w_{ad} \tag{2}$$

Additional fixed parameters in the AdEx model are C as the membrane capacitance, g_L as the leak conductance, E_L as the resting potential, and Δ_T as the slope factor. The parameter values are taken from Naud et al. [43] (see Tab.1 for parameter values).

Due to the chosen learning rules in the separate learning phase of the layer 4 model part, the excitatory

and inhibitory population consists of AdEx neurons following the implementation in Clopath et al. [44] (see Tab.1 for parameter values). In this slightly different neuron model, the membrane potential is extended with a depolarizing afterpotential (z), which increases after each spike by I_{sp} and decays with τ_z to zero (Eq.3). Additionally, the fixed spiking threshold is replaced by an adaptive threshold, which is set after each spike to V_{Tmax} and decays with a time constant of τ_{V_T} back to the lower value of V_{rest} (Eq.4).

$$\tau_z \frac{dz}{dt} = -z \tag{3}$$

$$\tau_{V_T} \frac{dV_T}{dt} = (V_T - V_{rest}) \tag{4}$$

	RGC and LGN cells	Cells in V1
Parameter	Value	Value
C	200 pF	281 pF
g_L	10 nS	30 nS
E_L	-58 mV	-70.6 mV
Δ_T	2 mV	2 mV
$\tau_{w_{ad}}$	120 ms	144 ms
a	0.03 nS	4.0 nS
b	100 pA	0.0805 pA
V_r	-46 mV	-70.6 mV
V_T	-50.4 mV	-
V_{rest}	-	-50.4 mV
V_{Tmax}	-	-30.4 mV
τ_{V_T}	-	50 ms
τ_z	-	40 ms

Table 1: Parameter for the AdEx neuron model in the LGN and RGC population shown in the left column. Values are chosen to implement a bursting behavior [43]. Right column shows parameter for the AdEx neuron model in the excitatory and inhibitory population.

2.2 Network modifications

To investigate how the circuit dynamics are influenced by intercortical inhibition or the temporal offset between lagged and non-lagged LGN cells, we measured the simple cell direction selectivity on five different modifications of the network, modifying the delay in the feedforward synapses of the RGC, the LGN responses and the intercortical inhibition (**Fig.2a**).

To study how the network dynamics influence the emergence of the STRFs, we modified the delay in the surround field of the retinal ganglion cells. Further, we add a delay of 50 ms to the response of 50% of the LGN cells to implement a temporal offset in the thalamocortical input to the simple cells.

The influence of the temporal offset and inhibition on the direction selectivity has been investigated by the following modifications: In the first modification, all LGN cells respond at the same time (so no lagged LGN cells exist) and intercortical inhibition is not present in the network. For the second modification we

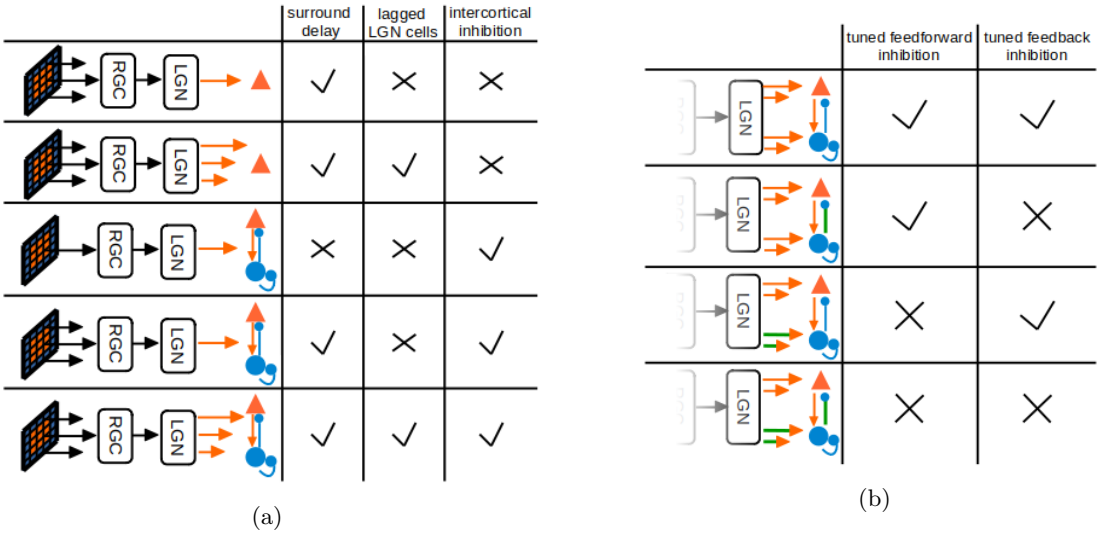

Figure 2: **Pictograms of network modifications to evaluate their influence on direction selectivity.** (a) Network modifications to analyze the influence on the emergence of STRFs and direction selectivity. We varied the delay in the surround field of the RGC receptive fields, adding lagged cells to the LGN population and adding tuned intercortical inhibition. (b) Network modifications to analyze the influence of tuned feedforward and feedback inhibition on direction selectivity. While Orange arrows indicating tuned excitatory and blue arrows tuned inhibitory synapses, green arrows indicating connections that are shuffled to remove the structure of the specific connection. Staggered arrows indicating a delay in either the synapses or the neuron responses.

added lagged LGN cells to implement a temporal offset in the thalamocortical input stream, still without intercortical inhibition. Finally, we added tuned intercortical inhibition to the network and measured direction selectivity once with and once without lagged LGN cells.

To evaluate the influence of tuned intercortical inhibition on direction selectivity, we compare the network with tuned feedforward and feedback inhibition with three variants in which in some connections the tuning has been removed by shuffling the weights (**Fig.2b**). For the first variant, we removed the tuning in the feedback synapses from the inhibitory to the excitatory population. In the second variant, we removed the tuning in all excitatory synapses to the inhibitory population (from LGN as well as from the excitatory population), removing the spatial tuning of inhibitory neurons. Finally, we removed the tuning of all synapses to the inhibitory population and in the inhibitory feedback synapses. We did not untune the lateral inhibitory synapses within the inhibitory population, as previous work demonstrated that this will not have a strong effect on the simple cell responses [28].

2.3 Analysis methods

2.3.1 Spatiotemporal receptive fields

An established method for measuring the spatiotemporal receptive fields is the reverse correlation technique [8, 10, 9, 12]. We presented 200,000 randomly chosen bright or dark bars and recorded all time points

where a cell spiked during the presentation. Each bar was presented for 50 ms, its position was chosen randomly and the size varied between one and eight pixels in height and width. To obtain a 3D-response profile, we summed over the stimuli presented in the last 300 ms before a spike occurred and divided it by the number of spikes.

2.3.2 Quantify the inseparability of STRFs

To measure if the STRF of an excitatory cell is either separable or inseparable, we first calculated the frequency spectrum of each neuron via a Fourier transformation [10]. The amplitudes for positive and negative temporal frequencies should be equal for separable STRFs, and different for inseparable STRFs [10, 12, 6]. Thus, the difference between the temporal frequency amplitudes (TFD) quantifies the "inseparability" of the excitatory cells (see **Eq.5**), with A_p as the maximum amplitude value of positive frequency and A_n maximum amplitude of the negative frequencies. For separable STRF the TFD value is zero, whereas a value closer to one indicates an inseparable STRF.

$$\mathrm{TFD} = \frac{|A_p - A_n|}{max(A_p, A_n)} \tag{5}$$

2.3.3 Direction selectivity index

Direction selectivity is determined by using moving sinusoidal gratings [45, 5]. To find the optimal moving sinus grating for each cell, we varied the spatial frequency from 1 *cycles/image* up to 5 *cycles/image* and the temporal frequency from 2 *cycles/second* up to 6 *cycles/second*. Each grating was presented for 20 different movement directions and moved for 3000 ms in each direction. We also determined the preferred orientation of each cell with a static, non-moving sinus grating. The preferred orientation together with the preferred spatial and temporal frequency is used to determine the two directions where the cell shows its highest response (preferred direction) and its lowest response (null or non-preferred direction). We calculate the direction selectivity index (DSI) as proposed by Peterson et al. [45] (Eq.6):

$$\mathrm{DSI} = 1 - \frac{R_0}{R_p} \tag{6}$$

R_p is the neuron activity (number of spikes) in the direction with the highest activity (preferred direction) and R_0 is the neuron activity in the null (opposite) direction. Cells that are highly selective for one direction have a DSI closer to 1, and cells that a less selective for one direction have a DSI close to 0.

2.3.4 Temporal offset between excitation and inhibition

To calculate the temporal offset (Δ_T) between the excitatory and inhibitory input currents we calculated the Pearson correlation between the excitatory input current and a time-shifted version of the inhibitory

input current, similar to the method described in Okun and Lampl [46]. Therefore, the inhibitory current is shifted in time from -20 ms up to + 20 ms. The time shift where the correlation value is highest is used as Δ_T to determine the arrival of inhibition relative to the arrival of excitation. A negative value of Δ_T indicates a delayed arrival of the original inhibitory current, whereas a positive value indicates that the inhibitory input arrives earlier than the excitatory one.

To relate the temporal dynamics of the inhibitory cells to the similarity between their receptive field and those of excitatory cells, we first calculated the receptive field similarity between all excitatory and inhibitory cells (see below). Second, for each excitatory cell, we binned inhibitory neurons with respect to their similarity to five bins. Third, we calculated the peristimulus time histogram (with a time bin of 2 ms and over 5 stimulus repetitions) for each inhibitory neuron in one bin and multiplied it by the weight value of the inhibitory feedback synapse. By averaging over all inhibitory cells in each bin, we calculate the expected inhibition an excitatory cell receives over the time of a stimulus presentation. Finally, we averaged the excitatory input current over 2 ms time bins and calculated the temporal offset as described above.

2.3.5 Selectivity similarity

To measure if a pair of excitatory and inhibitory cells are similar in their selectivity, we used the feedforward weights (excitatory input synapses from the LGN) and calculated the cosine between them (see **Eq.7**), with W_i as the feedforward weight vector of the excitatory neuron i and W_j as the feedforward weight vector of the inhibitory neuron j.

$$cos(\phi_{i,j}) = \frac{W_i \cdot W_j}{|W_i||W_j|} \tag{7}$$

3 Results

3.1 Surround to center delay leads to spatiotemporal receptive fields

Our results show that the structure of a spatiotemporal receptive field (STRF) depends on the surround delay of the ganglion cell receptive field and the temporal offset between lagged and non-lagged LGN cells (**Fig. 3**). Adding a delay of 30 ms to 50 ms to the surround field of the ganglion cells leads to a polarity flip of the simple cell receptive fields along the time axis in the STRF, typical for separable STRFs [10] (**Fig. 4**). An additional lag of 50 ms in the responses of 50% randomly chosen LGN cells leads to the emergence of an inseparable STRF profile (**Fig. 3**).

Data suggests, that the frequency spectrum of a separable and inseparable STRF differ in terms of the amplitudes for the negative and positive temporal frequencies [10, 12, 6]. For cells with a separable

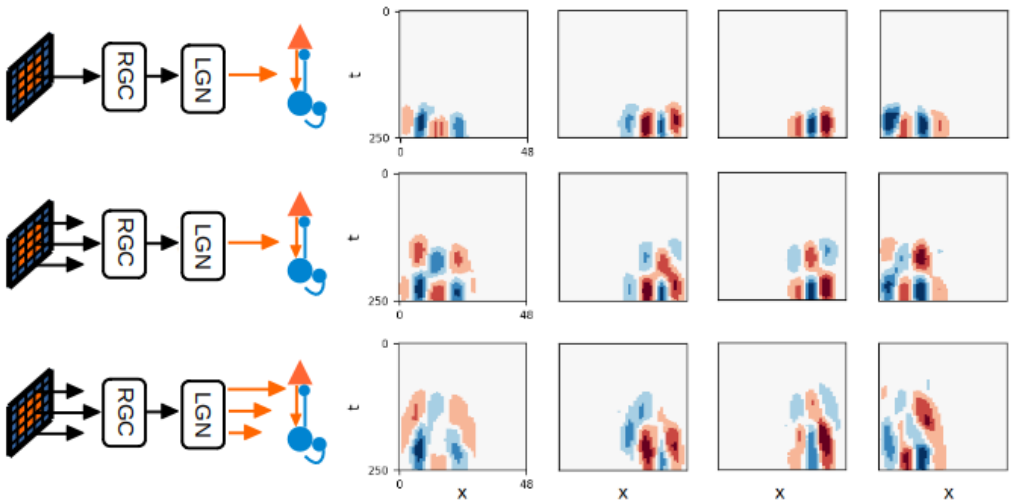

Figure 3: **Spatiotemporal receptive fields.** Each column shows the spatiotemporal receptive field (STRF) of one simple cell with different network configurations. If there is either a delay in the RGC surround field or a delay in the response of the LGN cells, there is no typical dynamic in the STRF (first row). With a delay in the RGC surround fields, separable STRFs emerge (second row). With a delay in the RGC surround fields and a lagged response for 50% of the LGN cells, the STRFs become more inseparable (third row).

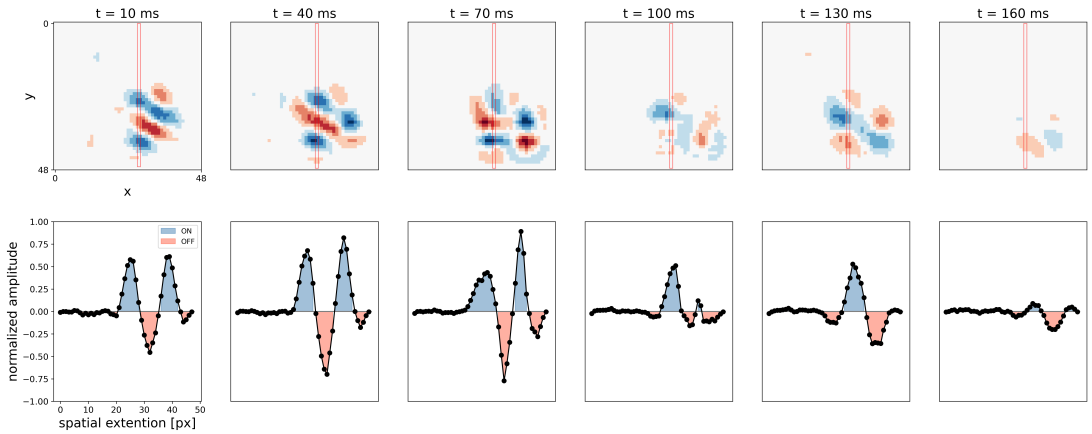

Figure 4: **Temporal change of simple cells receptive fields. Top:** Spatial receptive field of a randomly chosen neuron, on different time steps, relative to neurons spike. **Bottom**: Normalized profile of the spatial receptive field, relative to neurons spike. The red rectangle in the corresponding image above indicates the position of the profile.

STRF, the amplitudes for positive and negative temporal frequencies are equal, whereas the amplitudes for an inseparable STRF differ.

We calculated the frequency spectrum of all STRFs in the model with and without lagged LGN cells, respectively, and observed that the amplitudes are equal for a separable STRF (**Fig.5a**) and differ for a more inseparable STRF (**Fig.5b**). To quantify the "inseparability" of each STRF, we calculated the difference between the amplitudes of temporal frequencies (TFD). If the TFD value is closer to zero, it indicates a rather separable STRF and a value closer to one indicates a rather inseparable STRF (see **Eq.**

5). The TFD allows us to measure the effect of lagged LGN cells on the resulting distribution of separable and inseparable cells. We observe that without lagged LGN cells, most of the neurons have a low TFD, indicating that most neurons have separable STRFs (see **Fig.6a**). In contrast, lagged LGN cells lead to higher TFD values and so to more neurons with inseparable STRFs (see **Fig.6b**). Still, in either case we observe a range of TFD values, indicating a spectrum of different STRFs from total separable to clearly inseparable ones.

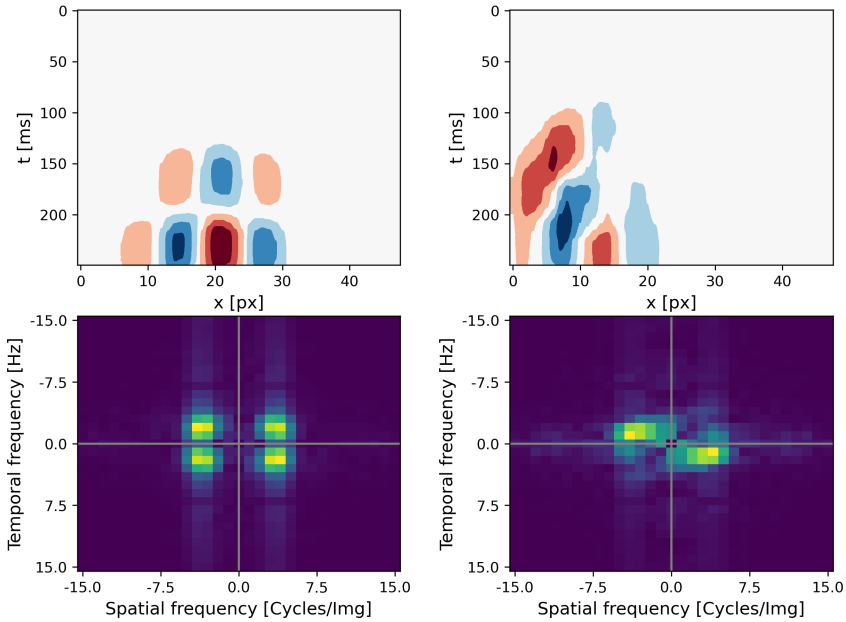

(a) (b)

Figure 5: **Inseparable STRF show different amplitudes for positive and negative temporal frequencies. (a)** Separable spatiotemporal receptive field of one exemplary cell (top) and the corresponding frequency spectrum (bottom). **(b)** Inseparable spatiotemporal receptive field of one exemplary cell (top) and the corresponding frequency spectrum (bottom), which does not show the symmetric distribution as the frequency spectrum of the separable STRF. The frequency spectrum is diagonal-symmetrical at the centered zero point.

3.2 Direction selectivity through lagged LGN cells and intercortical inhibition

We have seen an influence of lagged LGN cells on the inseparability of the STRF in our model. It has been suggested by previous model studies, that inseparable STRFs are more direction selective, linking lagged LGN directly to the emergence of direction selectivity [18, 16]. Furthermore, it has been suggested that intercortical inhibition could also cause direction selectivity [5, 23]. To analyze in our model the influence of both, lagged LGN cells and inhibition, we measured the direction selectivity of the excitatory neurons under varying model configurations.

We varied the model by removing the temporal lag in the response of the lagged LGN cells or by deactivating the intercortical inhibition but leaving the delay in the ganglion surround fields intact (**Fig.7**).

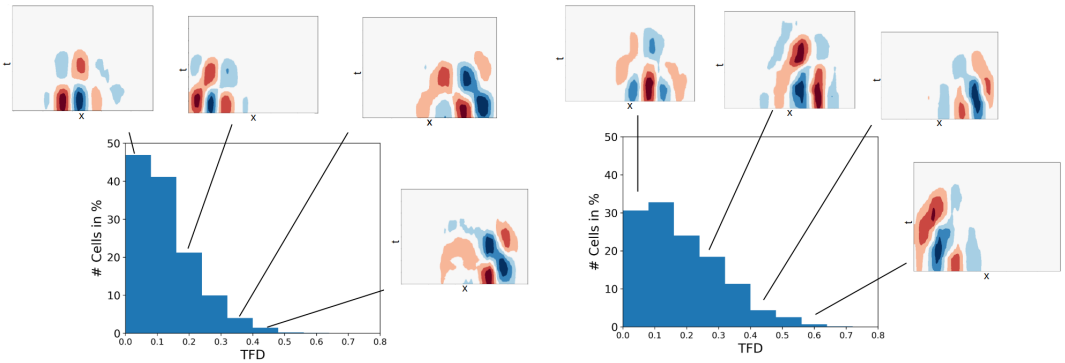

(a) (b)

Figure 6: **A more inseparable STRFs leads to a higher difference a the temporal frequency amplitudes (TFD). (a)** Without any lagged LGN cells, most of the STRFs have a small TFD value and rather separable STRFs. **(b)** If 50% of the cells in the LGN population are lagged cells with a delay of $50ms$, many simple cells tend to have inseparable STRFs indicated by a higher TFD value.

Without either lagged LGN cell or inhibition, we obverse that most of the simple cells show no or only weak direction selectivity. With 50% of the LGN populations being lagged cells (with a lagged response of 50 ms), but without inhibition, the DSI distribution did not vary. If the network contains no lagged LGN cells but active intercortical inhibition, more cells show a higher direction selectivity, leading to a more long-tailed distribution of the DSI. If both exist, lagged LGN cells and inhibition, even more neurons gain a higher direction selectivity, approaching a uniform distribution. These results suggest, that both, lagged LGN cells and inhibition, influence the emergence of direction selectivity. To analyze how both work together, we perform a qualitative evaluation by studying the response profile of four cells with different direction selectivity in the four different model configurations (see **Fig. 8**). The resulting response profiles show, that with blocked intercortical inhibition a broad tuning is observable, regardless of the lagged property in the LGN cells. However, intercortical inhibition without lagged LGN cells leads to a more symmetric (bidirectional) tuning, while additional lagged LGN cells lead to a dominant direction (unidirectional tuning).

3.2.1 Input offset leads to asynchronous inhibition

To better understand how inhibition and lagged cells support neuronal selectivity, we measured the temporal offset (ΔT) between the excitatory and inhibitory input current and grouped the simple cells along their DSI value into 5 groups in the model with lagged cells and inhibition.

We observe that for cells with lower DSI values (between 0 and 0.2), the offset (ΔT) for most of the cells is around -6 ms at the preferred stimulus direction (see **Fig. 9a**). A similar temporal offset is observable for the null direction, indicating, that the excitatory current arrives 6 ms before the inhibitory one for driving the neuron towards a spike, regardless of the stimulus direction. For cells with higher DSI,

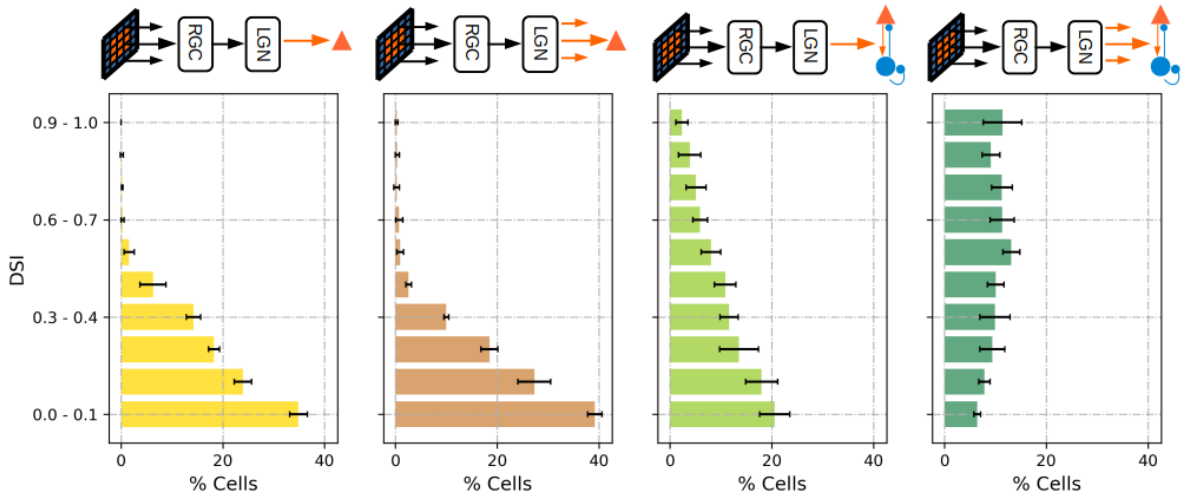

Figure 7: **Inhibition and lagged LGN cells contribute to direction selectivity in V1.** Percentage of simple cells in a certain range for the DSI. The length of each bar indicates the average percentage of cells over five network instances using different sets of pre-trained weights. The whiskers indicate the standard deviation over five network instances using a different set of pre-trained weights. Pictograms over the plots indicate lagged or non-lagged LGN cells (lagged: three orange arrows) or intercortical inhibition (blue lines) in the network. Without either intercortical inhibition or lagged LGN cells, the majority of simple cells showing no direction tuning (first plot on the left). With lagged LGN cells (but without inhibition), most simple cells are showing no direction tuning (second figure from left). With intercortical inhibition (but without lagged LGN cells), more cells show a weak to strong direction selectivity (third figure from left). With intercortical inhibition and lagged LGN cells, most of the cells show a strong unidirectional selectivity (fourth figure from left).

the temporal offset of the preferred direction changes to around -10 ms, indicating a longer temporal offset between the excitatory and inhibitory current, giving the cell enough time to spike before inhibition arrives, while on the null direction, the offset is close to 0 ms, indicating that the inhibitory and the excitatory currents arrive at nearly the same time to cancel each other out.

To understand how the temporal offset and the direction selectivity are influenced by lagged LGN cells, we measured for simple cells with a high direction selectivity how the temporal offset and the direction selectivity changes (Δ DSI) if the response of lagged LGN is not delayed any more. We observe that for cells with a high Δ DSI value, inhibition and excitation arrive more synchronously at the preferred direction if no lagged LGN cells exist, while with lagged LGN cells inhibition arrives later than excitation (see **Fig. 9c**). In the null direction, we observe a reverse trend. Cells with a high Δ DSI value show a smaller temporal offset with lagged LGN cells, while without lagged LGN cells the absolute temporal offset gets higher, indicating a larger temporal gap between the excitatory and inhibitory input current (see **Fig. 9d**). Further, we observe that the temporal offset between the input currents without lagged LGN cells is more similar in both directions (see **Fig. 9b**). This suggests, that without lagged cells, both input currents in the preferred and the null direction arrive at a similar time and lead to a similar response in both directions. This symmetry is broken by a delay in the response of the lagged cells, leading to a

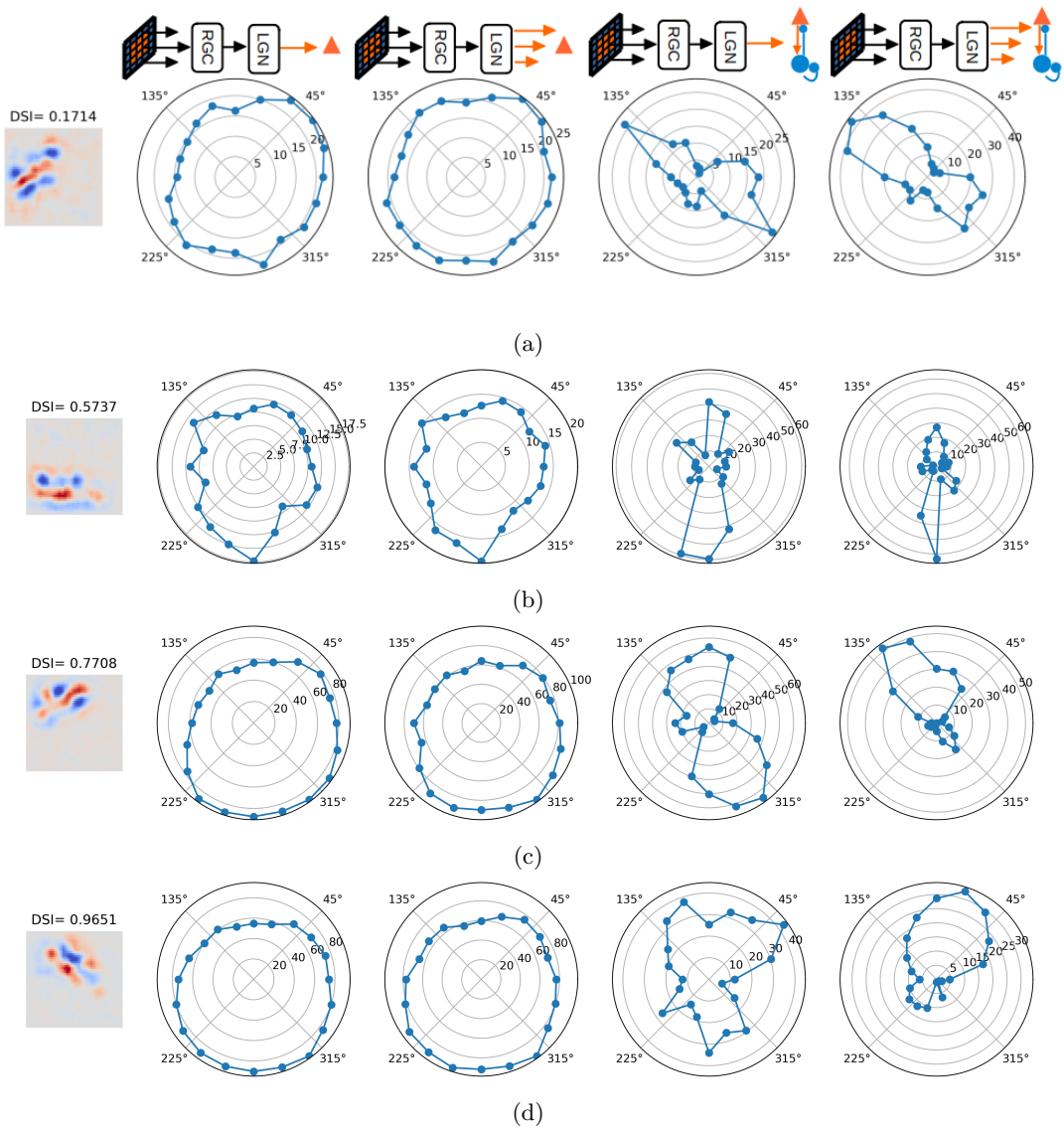

Figure 8: **Response profiles to moving sinusoidal gratings of four cells with different levels of direction selectivity and different model configurations.** Cells show a similar broadly tuned response profile in models without intercortical inhibition (first two columns). With inhibition (but without lagged LGN cells, third column), the response profile sharpens but is tuned to two opposing directions. With lagged LGN cells and inhibition (fourth column), the cells with a high DSI showed a clear preference for one of the two directions.

later arrival of inhibition at the preferred direction and a synchronous arrival of both input currents at the null direction.

3.2.2 Tuned inhibition improved direction selectivity

Due to the temporal offset, induced by the response delay of the lagged LGN cells, inhibition acts differently for the preferred direction compared to the null direction, leading to higher direction selectivity. However, as the pre-training on natural scenes leads to structured connectivity between the excitatory and inhibitory population, as well as to tuned inhibitory cells, circuit motifs may also influence the direction

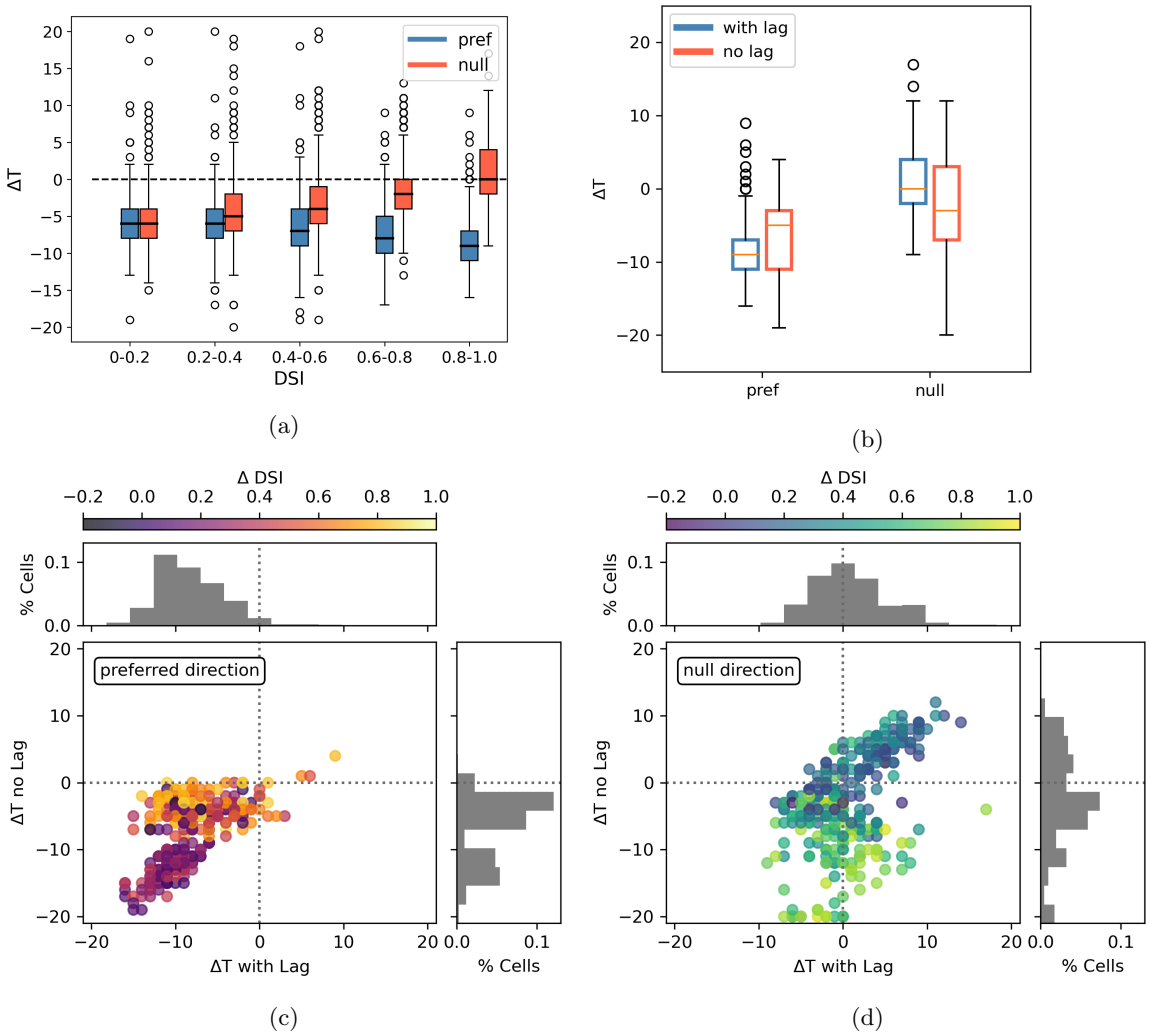

Figure 9: **Temporal offset between excitatory and inhibitory input current is different for cells with a high DSI.** ΔT marks the peak of the cross-correlation between the excitatory and inhibitory input currents to the simple cells. It indicates the offset between the excitatory and inhibitory current in ms. A negative ΔT means, that the inhibitory current arrives later than the excitatory one. (a) Temporal correlation between excitatory and inhibitory input currents as a function of DSI. For cells without a direction selectivity, the temporal offset for the preferred (blue) and non-preferred (orange) direction is equal (-6 ms). In cells with a high direction selectivity, the excitatory current arrives sooner than the inhibitory current at the preferred direction, otherwise, inhibition and excitation arrive at the same time. The black line indicates the median value. (b) Comparison of ΔT at the preferred direction and null direction for cells with a high direction selectivity with lagged LGN cells (blue) and without lagged LGN cells (red). With lagged LGN cells, the difference between the preferred and null direction is higher than without lagged LGN cells. (c) ΔT of cells that are highly direction selective with lagged LGN cells and without lagged LGN cells at the preferred direction. The color indicates the difference in the DSI between the model with lagged LGN cells and without. (d) ΔT of cells that are highly direction selective with lagged LGN cells and without lagged LGN cells at the null direction. The color indicates the difference in the DSI between the model with lagged LGN cells and without. Cells in (b), (c), and (d) are cells with a DSI > 0.8 in the model with intercortical inhibition and with lagged LGN cells.

selectivity. We calculated the DSI again for three model configurations: First, with a shuffled feedback connection from inhibition to excitation, excitatory neurons receive random feedback inhibition. Second,

the feed-forward weights (from LGN and from the excitatory population) to the inhibitory populations are shuffled, leading to untuned inhibitory cells. Third, inhibitory feedback and feed-forward weights to the inhibitory population are shuffled. By comparing the resulting DSI values with the standard model, we observe small changes if only the inhibitory feedback weights are shuffled (see **Fig.10**). In contrast to that, shuffling the feedforward inhibition (leading to unselective inhibitory neurons), a strong decrease of selectivity for most of the cells with a high direction selectivity is observable. This suggests that the temporal difference between the excitatory and inhibitory input currents depends on the tuning of inhibitory and excitatory cells.

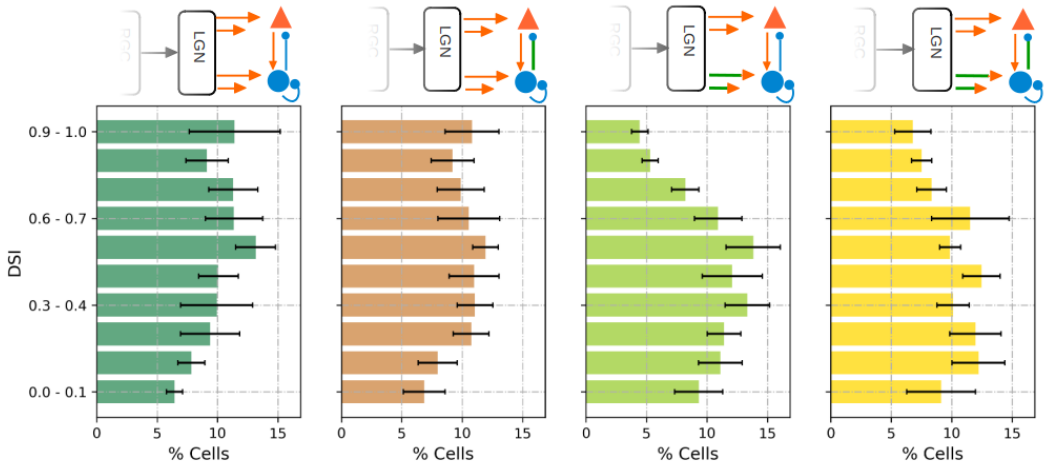

Figure 10: **Tuned feed-forward inhibition contributes to direction selectivity.** With tuned inter-cortical inhibition and with 50% lagged LGN cells with a delay of 50 ms, most of the cells show a high direction selectivity (first plot left). Untuned feedback inhibition does not change the DSI distribution (second plot from left). In contrast to that, untuned feed-forward inhibition leads to lower DSI values (third plot from left), and additional untuned feedback inhibition does not change the direction selectivity (fourth plot from left), indicating that tuned feed-forward inhibition mainly contributes to direction selectivity. The length of each bar indicates the average percentage of cells over five network instances. The whiskers indicate the standard deviation over five network instances.

To evaluate how the selectivity of excitatory and inhibitory neurons shape direction selectivity, we first calculated an approximated inhibitory current generated by each inhibitory neuron, which is sent to an excitatory neuron. For that, we multiplied the synaptic inhibitory feedback weight with the number of spikes in a time frame of 2 ms. Second, we calculated the temporal offset (respective to the ΔT as described above) between the excitatory input current of the excitatory cell and all approximated inhibitory currents. Third, we calculated the cosine similarity between the input synapses of all excitatory and inhibitory cells. Due to the fact, that the cell's selectivity and its receptive fields are mainly controlled by the thalamocortical input from lGN, measuring the cosine similarity can be used to determine how similar the receptive fields of excitatory and inhibitory cells are. While a value closer to one indicates, that the inhibitory neurons have a similar orientation, and phase, and are in the same position in the

input space, a negative similarity value indicates a receptive field with the same position and orientation but with a reverse phase. A similarity value around zero indicates mainly a receptive field with a different position at the input space (see **S1**). The cosine similarity is used to group the inhibitory cells in relation to the receptive field similarity of an excitatory neuron, to evaluate how the temporal offset between the excitatory and inhibitory input current is influenced by the receptive field similarity.

We observe that for highly direction-selective cells the input currents from inhibitory cells with a cosine around zero (e.g., inhibitory cells at a different position) have a temporal offset of ΔT = -4 ms, on average at the preferred direction and a $\Delta T = +5$ ms at the null direction (see **Fig.11**). This indicates that inhibitory neurons in a different position spiked later in the preferred direction and earlier in the null direction. In contrast to that, the inhibitory currents from cells at the same position but with a similar orientation (what is true for inhibitory cells with a cosine around -0.8 and 0.8) arrive on average at a similar time as the excitatory input current regardless of the direction. For excitatory cells that do not show any level of direction selectivity (DSI < 0.2), the temporal offset is on average around zero, for both directions. These results indicate that the positional relation between excitatory and inhibitory cells also influences the direction selectivity.

4 Discussion

Ganglion cell surround delay as the origin of spatiotemporal receptive fields A large fraction of models implements spatiotemporal receptive fields (STRFs) by the combination of a spatial activation function and a non-linear bi-phasic function for the temporal behavior, either directly in the simple cell model [47, 48, 49], in the model for LGN cells [16, 17, 18, 25, 26], or in the retinal ganglion cell model [50, 51]. Despite their success in modeling the functional components of STRFs and providing suitable models for further analysis (like for direction selectivity or the analysis of higher cortical areas), they do not explain how STRFs emerge through network circuit motifs.

To propose a possible neuronal mechanism for the emergence of STRFs, we demonstrate how a delay in the surround field of the retinal ganglion cells enables the emergence of STRFs. It has been suggested in previous studies, that a good fit of STRFs for retinal ganglion cells or LGN can be achieved by extending the classical DoG receptive field to simulate a delay in the surround field [29, 52, 13]. While Enroth-Cugell et al. [29] and Dawis et al. [52] changed the DoG to simulate the functional implication of a delay in the frequency domain, Cai et al. [13] demonstrated how a delay in the temporal function for the surround field leads to LGN STRFs. Instead of an additional temporal function to model the temporal dynamics of the ganglion cell responses, we delayed the transmission of the surround inputs directly in the synapse objects of the ANNarchy simulator. Due to this, we model the neuronal responses in all populations only with the biologically plausible adaptive exponential integrate-and-fire model, leading to STRFs for V1

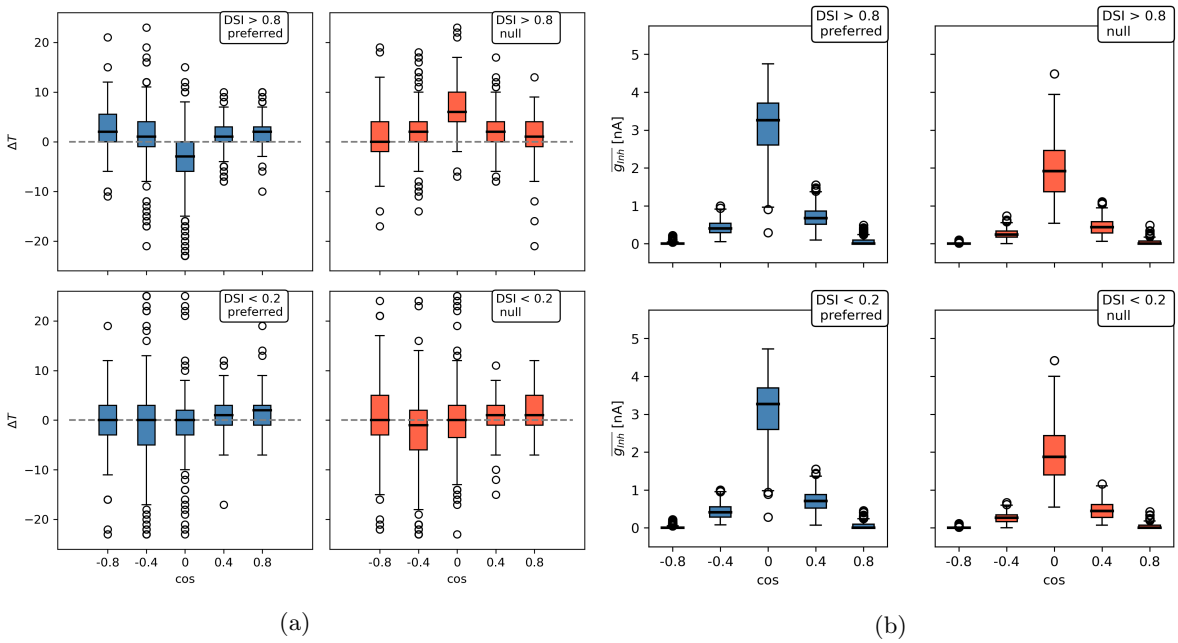

Figure 11: **Tuned inhibition controls direction selectivity.** **(a)** Cross-correlation between the excitatory input current and the approximated inhibitory input current as a function of the receptive field cosine. The ΔT marks the temporal shift in the inhibitory current that leads to the maximum correlation. For cells with a DSI > 0.8, the corresponding inhibitory current from cells with a cosine around zero shows a negative ΔT, indicating that the current arrives later than the excitatory current. While the inhibitory feedback from cells with a higher cosine value is nearly simultaneous. In contrast to that, in the null direction, the inhibitory current from cells with a cosine around zero arrives sooner than the excitatory input current. If the DSI < 0.2, the temporal difference between the cells is for both directions, preferred and null, similar.
(b) Average approximated inhibitory current over the complete stimulus presentation as a function of the receptive field cosine. Independently of the DSI and the direction, most of the inhibitory current is generated by inhibitory cells with a receptive field having a different orientation and a spatial offset to the postsynaptic excitatory cell. In the average inhibitory current, there is no difference between cells with a high or low DSI.
Top row, data for excitatory cells with a DSI > 0.8, and at the bottom row, data is presented for excitatory cells with a DSI < 0.2. On the left, data presented for the preferred orientation (in blue), and on the right data presented for the null direction (in red).

simple cells and also for cells in the LGN population (**Fig. S2**) as reported in cat [9]. The assumption for the existence of surround delays is supported by different experimental studies, which reported a delayed response of the ganglion surround field relative to the center for different mammalian [34] and non-mammalian species [35, 53]. It may emerge from a delay in the surround field of bipolar cells as a consequence of the interaction with horizontal cells in the outer retina [36], or by amacrine cells in the inner retina which shape the spatial selectivity of bipolar and ganglion cells, as well as influence their temporal dynamics [31, 54].

Lagged LGN cells lead to more inseparable STRFs A STRF is called separable if its space-time profile can be described by two separable functions for the space and time dimensions, otherwise, it is called

inseparable [47, 10, 11, 12]. It has been assumed previously, that temporal offset created by the combined response of non-lagged and lagged LGN cells creates the inseparability of STRFs [55, 11]. Studies in the mammalian visual cortex showed that STRFs of simple cells lay in a spectrum from clearly separable to strongly inseparable [56]. We proposed here a new method to measure the grade of inseparability by calculating the difference between the temporal frequency amplitudes in the Fourier spectrum. With this temporal frequency amplitude difference (TFD), we quantify the numbers of simple cells with a specific level of inseparability in the corresponding STRF, where a value closer to zero indicates a separable STRF and a value closer to one indicates a more inseparable STRF. Our results show, that in the absence of lagged LGN cells, a majority of simple cells have a TFD < 0.2 and thus, a separable STRF. Adding a delay to the response of 50% of the lagged LGN cells results in an increase of the TFD value for most of the cells, accompanied with the emergence of more inseparable STRFs for these cells.

Inhibition together with lagged LGN cells leading to direction selectivity Lagged cells have been found in the lateral geniculate nucleus of cats [57, 15, 13, 58, 38], monkeys [59, 60], and mice [61]. Different model studies showed how the combination of the shifted input through non-lagged and lagged LGN cells creates a temporal offset in the input to layer 4, that can be responsible for the emergence of direction selectivity, even without inhibition in layer 4 [16, 19, 26, 62].

It has been suggested, that the temporal offset in the input stream from LGN to V1 could not only be implemented through non-lagged and lagged LGN cells but also by transient and sustained LGN cells [63]. While the existence of these cells is well known [64, 59, 58], their relevance for direction selectivity in the visual cortex remains unclear. It has been shown in mice's visual cortex, that direction-selective cells receive input from LGN cells with a transient response profile and from cells with a sustained response profile [62]. A potential role of these LGN cells for direction selectivity as been suggested [63] as well as neglected [65] by recent model studies.

Besides the properties of LGN cells, researchers pointed out an effect of intracortical inhibition on direction selectivity in the visual systems of cats [66, 6], mice [20, 21, 67], ferrets [7], and monkeys [68], even questioning the role of lagged LGN cells through the need for exact timing of lagged and non-lagged cells to achieve direction selectivity [5]. It has also been shown in model studies, that direction selectivity could emerge through intracortical inhibition, without the need for lagged LGN cells [22, 23].

Our model simulations support the assumption that both, lagged LGN cells (or related mechanisms) and intracortical inhibition, has to taken into account to explain direction selectivity. While previous models suggest that the thalamocortical input provides a basis direction selectivity, which is enhanced through intercortical inhibition [25, 63], our model simulations suggest an alternative explanation. Our results show, that simple cells show a clear orientation selectivity through intercortical inhibition, but no direction selectivity, if lagged LGN cells are missing, due to a similar arrival of excitatory feedforward

and inhibitory feedback currents for both directions. Direction selectivity in our model increases if the temporal offset introduced by lagged LGN cells leads to a delayed response of either inhibitory cells or excitatory cells to break the synchronicity between both input currents at the preferred and null direction in favor of one of them.

Orientation and spatial offset as source of asymmetric inhibition While our results show that the temporal offset between non-lagged and lagged LGN cells provides an advantage for one direction, we observed that direction selectivity also benefits from tuned feedforward inhibition. Inhibitory cells with different orientations and different spatial positions contribute by sending their inhibitory currents early at the null direction to cancel out the excitatory input current and only later at the preferred direction, improving direction selectivity. This asymmetric inhibition has been found in the visual cortex of monkeys [68], cats [5], and mice [21]. Furthermore, various model studies investigated the influence of asymmetric inhibition on direction selectivity [25] and even demonstrated how intercortical inhibition leads to direction selectivity without a temporal offset in the LGN feedforward path [23].

By demonstrating that direction selectivity emerges through inhibitory cells with the same orientation and either the same or the opposite phase, Ursino et al. [25] suggested that the phase of the inhibitory neuron in relation to the excitatory neuron is not important. Supporting this claim, our results show that the inhibitory neurons with the same orientation and the same phase as well as the opposite phase spike nearly simultaneously with the excitatory cell at the preferred and null direction, supporting the assumption that the inhibitory phase is irrelevant for direction selectivity. In a recent model study, Freeman [23] demonstrated in a rate-coded orientation map model trained by a developmental procedure how direction selectivity emerges through intercortical inhibition alone, without a temporal offset in the thalamocortical path. In their model simple cells gain direction selectivity through neighboring inhibitory neurons, which are selective for different orientations. Due to the different orientations, the averaged spatial receptive field of the inhibitory neurons shows a spatial offset from the receptive field of the simple cell. This leads to an inhomogeneous inhibitory input current in time, arriving later at the preferred direction and earlier at the non-preferred direction. Our results demonstrate, how the temporal offset in the thalamocortical feedforward path leads to a basic level of direction selectivity, which is increased through tuned inhibition. Similar to the findings of Freeman [23], we observe in our network that the accumulated input from inhibitory cells with a spatial offset and different orientations arrives delayed in the preferred direction and early on in the non-preferred direction. However, the model of Freeman [23] did not contain any spatiotemporal dynamics in the simple cell population or a temporal offset in the thalamocortical feedforward path, leaving it open to how these circuit motifs would influence the direction selectivity. Beyond the study of Freeman [23], our network demonstrated how direction selectivity is influenced by the combined effect of a temporal offset in the thalamocortical path and tuned intercortical

inhibition.

Conclusion In this study, we presented how the incorporation of different network motifs and neuronal dynamics in a spiking neural network shape the characteristics of spatiotemporal receptive fields (STRFs) and enable direction selectivity for V1 simple cells (see **Fig. 12** for a summary). We demonstrated how a delay in the surrounding field of ganglion cells solely leads to the emergence of separable STRFs for cells in the LGN, as well as for V1 simple cells. Further, we showed how the addition of a response delay to 50% of the LGN cells leads to the emergence of inseparable STRFs in the V1 simple cell population. We systematically analyzed the influence of the temporal offset in the thalamocortical input path and the influence of tuned and non-tuned intercortical inhibition on direction selectivity. Direction selectivity emerges due to two mechanisms in our network: First, tuned lateral inhibition is mainly influenced by the preferred orientation and spatial offset, leading to a weak direction selectivity of most cells. Together with the second mechanism, the temporal offset caused by non-lagged and lagged LGN cells, gives an additional temporal advantage and together with inhibition, controls the response in the preferred and null direction.

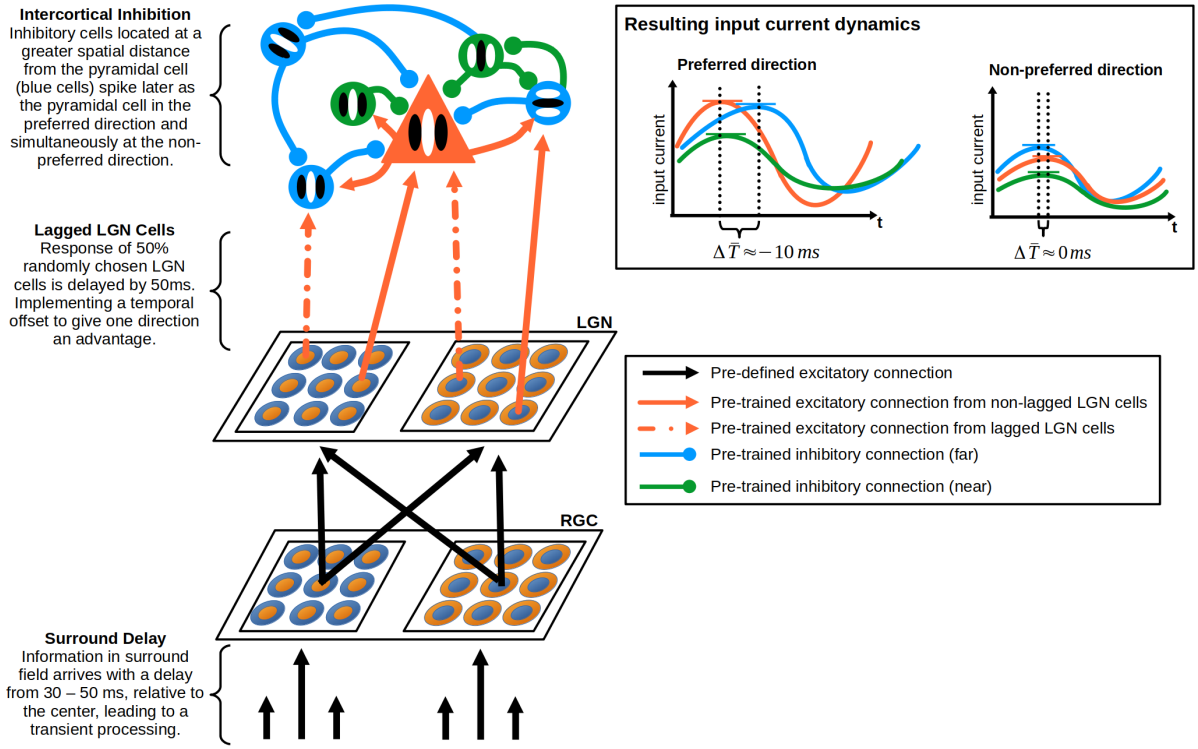

Figure 12: **Network motifs and their role for direction selectivity.** Due to the delays in the surround field of the retinal ganglion cells, spatial information of the centre and surround are decoupled in time, leading to transient processing in the next layer. A temporal offset between lagged and non-lagged LGN cells leads to a delayed response and dependent on the thalamocortical connectivity will give one direction a temporal advantage. Tuned intercortical inhibition increases direction selectivity, as inhibitory cells with a higher spatial offset of their receptive field and a different orientation spike differently at the preferred and non-preferred direction. Together, these network motifs influence the temporal dynamics of excitatory and inhibitory input currents to enable direction selectivity.

Acknowledgment

This research has been funded by the Saxony State Ministry of Science and Art (SMWK3-7304/35/3-2021/4819) research initiative "Instant Teaming between Humans and Production Systems". Open Access has been funded by the Deutsche Forschungsgemeinschaft (DFG, German Research Foundation) project number 491193532 and the Chemnitz University of Technology.

Author Contributions

Conceptualization	René Larisch
Formal Analysis	René Larisch
Funding Acquisition	Fred H. Hamker
Investigation	René Larisch
Methodology	René Larisch
Resources	Fred H. Hamker
Software	René Larisch
Validation	René Larisch
Visualization	René Larisch
Writing - Original Draft Preparation	René Larisch
Writing - Review & Editing	Fred H. Hamker, René Larisch

Declaration of Interest

The authors declare no competing interests.

References

[1] D. H. Hubel and T. N. Wiesel. Receptive fields of single neurones in the cat's striate cortex. *The Journal of Physiology*, 148(3):574–591, 1959. doi: https://doi.org/10.1113/jphysiol.1959.sp006308. URL `https://physoc.onlinelibrary.wiley.com/doi/abs/10.1113/jphysiol.1959.sp006308`.

[2] D. H. Hubel and T. N. Wiesel. Receptive fields and functional architecture of monkey striate cortex. *The Journal of Physiology*, 195(1):215–243, 1968. doi: https://doi.org/10.1113/jphysiol.1968.sp008455. URL `https://physoc.onlinelibrary.wiley.com/doi/abs/10.1113/jphysiol.1968.sp008455`.

[3] David Rose and Colin Blakemore. An analysis of orientation selectivity in the cat's visual cortex. *Experimental Brain Research*, 20(1):1–17, Apr 1974. ISSN 1432-1106. doi: 10.1007/BF00239014. URL `https://doi.org/10.1007/BF00239014`.

[4] N. E. Berman, M. E. Wilkes, and B. R. Payne. Organization of orientation and direction selectivity

in areas 17 and 18 of cat cerebral cortex. *Journal of Neurophysiology*, 58(4):676–699, 1987. doi: 10.1152/jn.1987.58.4.676. URL https://doi.org/10.1152/jn.1987.58.4.676. PMID: 3316523.

[5] Nicholas J. Priebe and David Ferster. Direction selectivity of excitation and inhibition in simple cells of the cat primary visual cortex. *Neuron*, 45(1):133–145, 2005. ISSN 0896-6273. doi: https://doi.org/10.1016/j.neuron.2004.12.024. URL https://www.sciencedirect.com/science/article/pii/S0896627304008402.

[6] Taekjun Kim and Ralph D. Freeman. Direction selectivity of neurons in the visual cortex is non-linear and lamina-dependent. *European Journal of Neuroscience*, 43(10):1389–1399, 2016. doi: https://doi.org/10.1111/ejn.13223. URL https://onlinelibrary.wiley.com/doi/abs/10.1111/ejn.13223.

[7] Daniel E. Wilson, Benjamin Scholl, and David Fitzpatrick. Differential tuning of excitation and inhibition shapes direction selectivity in ferret visual cortex. *Nature*, 560(7716):97–101, Aug 2018. ISSN 1476-4687. doi: 10.1038/s41586-018-0354-1. URL https://doi.org/10.1038/s41586-018-0354-1.

[8] Judith McLean and Larry A. Palmer. Contribution of linear spatiotemporal receptive field structure to velocity selectivity of simple cells in area 17 of cat. *Vision Research*, 29(6):675–679, 1989. ISSN 0042-6989. doi: https://doi.org/10.1016/0042-6989(89)90029-1. URL https://www.sciencedirect.com/science/article/pii/0042698989900291.

[9] Gregory C. DeAngelis, Izumi Ohzawa, and Ralph D. Freeman. Receptive-field dynamics in the central visual pathways. *Trends in Neurosciences*, 18(10):451 – 458, 1995. ISSN 0166-2236. doi: https://doi.org/10.1016/0166-2236(95)94496-R. URL http://www.sciencedirect.com/science/article/pii/016622369594496R.

[10] G. C. DeAngelis, I. Ohzawa, and R. D. Freeman. Spatiotemporal organization of simple-cell receptive fields in the cat's striate cortex. ii. linearity of temporal and spatial summation. *Journal of Neurophysiology*, 69(4):1118–1135, 1993. doi: 10.1152/jn.1993.69.4.1118. URL https://doi.org/10.1152/jn.1993.69.4.1118. PMID: 8492152.

[11] J. McLean, S. Raab, and L. A. Palmer. Contribution of linear mechanisms to the specification of local motion by simple cells in areas 17 and 18 of the cat. *Visual Neuroscience*, 11(2):271–294, 1994. doi: 10.1017/S0952523800001632. URL https://doi.org/10.1017/S0952523800001632.

[12] I. Ohzawa, G. C. DeAngelis, and R. D. Freeman. Encoding of binocular disparity by simple cells in the cat's visual cortex. *Journal of Neurophysiology*, 75(5):1779–1805, 1996. doi: 10.1152/jn.1996.75.5.1779. URL https://doi.org/10.1152/jn.1996.75.5.1779. PMID: 8734580.

[13] Daqing Cai, Gregory C. Deangelis, and Ralph D. Freeman. Spatiotemporal receptive field organization in the lateral geniculate nucleus of cats and kittens. *Journal of Neurophysiology*, 78(2):1045–1061, 1997. doi: 10.1152/jn.1997.78.2.1045. URL https://doi.org/10.1152/jn.1997.78.2.1045. PMID: 9307134.

[14] Naofumi Suematsu, Tomoyuki Naito, Tomomitsu Miyoshi, Hajime Sawai, and Hiromichi Sato. Spatiotemporal receptive field structures in retinogeniculate connections of cat. *Frontiers in Systems Neuroscience*, 7:103, 2013. ISSN 1662-5137. doi: 10.3389/fnsys.2013.00103. URL https://www.frontiersin.org/article/10.3389/fnsys.2013.00103.

[15] A. B. Saul and A. L. Humphrey. Spatial and temporal response properties of lagged and nonlagged cells in cat lateral geniculate nucleus. *Journal of Neurophysiology*, 64(1):206–224, 1990. doi: 10.1152/jn.1990.64.1.206. URL https://doi.org/10.1152/jn.1990.64.1.206. PMID: 2388066.

[16] S. Wimbauer, O. G. Wenisch, K. D. Miller, and J. L. van Hemmen. Development of spatiotemporal receptive fields of simple cells: I. model formulation. *Biological Cybernetics*, 77(6):453–461, Dec 1997. ISSN 1432-0770. doi: 10.1007/s004220050405. URL https://doi.org/10.1007/s004220050405.

[17] Takashi Hamada, Masaki Yamashima, and Kazunori Kato. A ring model for spatiotemporal properties of simple cells in the visual cortex. *Biological Cybernetics*, 77(4):225–233, Oct 1997. ISSN 1432-0770. doi: 10.1007/s004220050383. URL https://doi.org/10.1007/s004220050383.

[18] Masanobu Miyashita, Dae-Shik Kim, and Shigeru Tanaka. Cortical direction selectivity without directional experience. *NeuroReport*, 8(5), 1997. ISSN 0959-4965. URL https://journals.lww.com/neuroreport/Fulltext/1997/03240/Cortical_direction_selectivity_without_directional.26.aspx.

[19] S. Wimbauer, O. G. Wenisch, J. L. van Hemmen, and K. D. Miller. Development of spatiotemporal receptive fields of simple cells: Ii. simulation and analysis. *Biological Cybernetics*, 77(6):463–477, Dec 1997. ISSN 1432-0770. doi: 10.1007/s004220050406. URL https://doi.org/10.1007/s004220050406.

[20] Seung-Hee Lee, Alex C. Kwan, Siyu Zhang, Victoria Phoumthipphavong, John G. Flannery, Sotiris C. Masmanidis, Hiroki Taniguchi, Z. Josh Huang, Feng Zhang, Edward S. Boyden, Karl Deisseroth, and Yang Dan. Activation of specific interneurons improves v1 feature selectivity and visual perception. *Nature*, 488:379–383, 2012. doi: 10.1038/nature11312. URL https://doi.org/10.1038/nature11312.

[21] Ya-tang Li, Bao-hua Liu, Xiao-lin Chou, Li I. Zhang, and Huizhong Whit Tao. Strengthening of Direction Selectivity by Broadly Tuned and Spatiotemporally Slightly Offset Inhibition in Mouse Visual

Cortex. *Cerebral Cortex*, 25(9):2466–2477, 03 2014. ISSN 1047-3211. doi: 10.1093/cercor/bhu049. URL https://doi.org/10.1093/cercor/bhu049.

[22] Oliver G. Wenisch, Joachim Noll, and J. Leo van Hemmen. Spontaneously emerging direction selectivity maps in visual cortex through stdp. *Biological Cybernetics*, 93(4):239–247, Oct 2005. ISSN 1432-0770. doi: 10.1007/s00422-005-0006-z. URL https://doi.org/10.1007/s00422-005-0006-z.

[23] Alan W. Freeman. A model for the origin of motion direction selectivity in visual cortex. *Journal of Neuroscience*, 41(1):89–102, 2021. ISSN 0270-6474. doi: 10.1523/JNEUROSCI.1362-20.2020. URL https://www.jneurosci.org/content/41/1/89.

[24] G.E. La Cara, M. Ritrovato, and M. Ursino. A model of direction selectivity in cortical simple cells based on lagged thalamic input and intracortical feedback. In *Proceedings of the 25th Annual International Conference of the IEEE Engineering in Medicine and Biology Society (IEEE Cat. No.03CH37439)*, volume 2, pages 1889–1892 Vol.2, 2003. doi: 10.1109/IEMBS.2003.1279788. URL https://doi.org/10.1109/IEMBS.2003.1279788.

[25] Mauro Ursino, Giuseppe-Emiliano La Cara, and Matteo Ritrovato. Direction selectivity of simple cells in the primary visual cortex: Comparison of two alternative mathematical models. i: Response to drifting gratings. *Computers in Biology and Medicine*, 37(3):398–414, 2007. ISSN 0010-4825. doi: https://doi.org/10.1016/j.compbiomed.2006.05.002. URL https://www.sciencedirect.com/science/article/pii/S0010482506000758.

[26] Kenji Okajima. Spatiotemporal receptive fields of direction selective cells self-organized by an infomax-based learning model. *Neurocomputing*, 129:548–555, 2014. ISSN 0925-2312. doi: https://doi.org/10.1016/j.neucom.2013.09.004. URL https://www.sciencedirect.com/science/article/pii/S0925231213008965.

[27] Julien Vitay, Helge Dinkelbach, and Fred Hamker. Annarchy: a code generation approach to neural simulations on parallel hardware. *Frontiers in Neuroinformatics*, 9:19, 2015. ISSN 1662-5196. doi: 10.3389/fninf.2015.00019. URL https://www.frontiersin.org/article/10.3389/fninf.2015.00019.

[28] René Larisch, Lorenz Gönner, Michael Teichmann, and Fred H. Hamker. Sensory coding and contrast invariance emerge from the control of plastic inhibition over emergent selectivity. *PLOS Computational Biology*, 17(11):1–37, 11 2021. doi: 10.1371/journal.pcbi.1009566. URL https://doi.org/10.1371/journal.pcbi.1009566.

[29] C Enroth-Cugell, J G Robson, D E Schweitzer-Tong, and A B Watson. Spatio-temporal interactions in cat retinal ganglion cells showing linear spatial summation. *The Journal of Physiology*, 341(1):279–307,

1983. doi: https://doi.org/10.1113/jphysiol.1983.sp014806. URL https://physoc.onlinelibrary.wiley.com/doi/abs/10.1113/jphysiol.1983.sp014806.

[30] J.B. Troy and T. Shou. The receptive fields of cat retinal ganglion cells in physiological and pathological states: where we are after half a century of research. *Progress in Retinal and Eye Research*, 21(3):263–302, 2002. ISSN 1350-9462. doi: https://doi.org/10.1016/S1350-9462(02)00002-2. URL https://www.sciencedirect.com/science/article/pii/S1350946202000022.

[31] Jeffrey S. Diamond. Inhibitory interneurons in the retina: Types, circuitry, and function. *Annual Review of Vision Science*, 3(1):1–24, 2017. doi: 10.1146/annurev-vision-102016-061345. URL https://doi.org/10.1146/annurev-vision-102016-061345. PMID: 28617659.

[32] Tom Baden, Thomas Euler, and Philipp Berens. Understanding the retinal basis of vision across species. *Nature Reviews Neuroscience*, 21(1):5–20, Jan 2020. ISSN 1471-0048. doi: 10.1038/s41583-019-0242-1. URL https://doi.org/10.1038/s41583-019-0242-1.

[33] Romain Brette and Wulfram Gerstner. Adaptive exponential integrate-and-fire model as an effective description of neuronal activity. *Journal of Neurophysiology*, 94(5):3637–3642, 2005. doi: 10.1152/jn.00686.2005. URL https://doi.org/10.1152/jn.00686.2005. PMID: 16014787.

[34] Yoichiro Tokutake and Michael A. Freed. Retinal ganglion cells – spatial organization of the receptive field reduces temporal redundancy. *European Journal of Neuroscience*, 28(5):914–923, 2008. doi: https://doi.org/10.1111/j.1460-9568.2008.06394.x. URL https://onlinelibrary.wiley.com/doi/abs/10.1111/j.1460-9568.2008.06394.x.

[35] Patrick K. Fahey and Dwight A. Burkhardt. Center-surround organization in bipolar cells: Symmetry for opposing contrasts. *Visual Neuroscience*, 20(1):1–10, 2003. doi: 10.1017/S0952523803201012. URL https://doi.org/10.1017/S0952523803201012.

[36] Dwight A. Burkhardt, Theodore M. Barroletti, and Wallace B. Thoreson. Center/surround organization of retinal bipolar cells: High correlation of fundamental responses of center and surround to sinusoidal contrasts. *Visual Neuroscience*, 28(3):183–192, 2011. doi: 10.1017/S0952523811000071. URL https://doi.org/10.1017/S0952523811000071.

[37] A.B. Saul. Lagged cells. *Neurosignals*, pages 209–225, 2008. doi: 10.1159/000111564. URL https://www.karger.com/DOI/10.1159/000111564.

[38] Leif E. Vigeland, Diego Contreras, and Larry A. Palmer. Synaptic mechanisms of temporal diversity in the lateral geniculate nucleus of the thalamus. *Journal of Neuroscience*, 33(5):1887–1896, 2013. ISSN 0270-6474. doi: 10.1523/JNEUROSCI.4046-12.2013. URL https://www.jneurosci.org/content/33/5/1887.

[39] P. L. A. Gabbott and P. Somogyi. Quantitative distribution of gaba-immunoreactive neurons in the visual cortex (area 17) of the cat. *Experimental Brain Research*, 61(2):323–331, Jan 1986. ISSN 1432-1106. doi: 10.1007/BF00239522. URL https://doi.org/10.1007/BF00239522.

[40] C. Beaulieu, Z. Kisvarday, P. Somogyi, M. Cynader, and A. Cowey. Quantitative distribution of gaba-immunopositive and-immunonegative neurons and synapses in the monkey striate cortex (area 17). *Cerebral Cortex*, 2(4):295–309, 1992. doi: 10.1093/cercor/2.4.295. URL +https://dx.doi.org/10.1093/cercor/2.4.295.

[41] Henry Markram, Maria Toledo-Rodriguez, Yun Wang, Anirudh Gupta, Gilad Silberberg, and Caizhi Wu. Interneurons of the neocortical inhibitory system. *Nature reviews. Neuroscience*, 5(10):793–807, 2004. ISSN 1471-003X. doi: 10.1038/nrn1519. URL https://dx.doi.org/10.1038/nrn1519.

[42] Bruno A. Olshausen and David J. Field. Emergence of simple-cell receptive field properties by learning a sparse code for natural images. *Nature*, 381(6583):607–609, 1996. ISSN 0028-0836. doi: 10.1038/381607a0. URL https://dx.doi.org/10.1038/381607a0.

[43] Richard Naud, Nicolas Marcille, Claudia Clopath, and Wulfram Gerstner. Firing patterns in the adaptive exponential integrate-and-fire model. *Biological Cybernetics*, 99(4):335, Nov 2008. ISSN 1432-0770. doi: 10.1007/s00422-008-0264-7. URL https://doi.org/10.1007/s00422-008-0264-7.

[44] Claudia Clopath, Lars Büsing, Eleni Vasilaki, and Wulfram Gerstner. Connectivity reflects coding: a model of voltage-based stdp with homeostasis. *Nature Neuroscience*, 13(3):344–352, 2010. ISSN 1097-6256. doi: 10.1038/nn.2479. URL https://www.nature.com/doifinder/10.1038/nn.2479.

[45] Matthew R. Peterson, Baowang Li, and Ralph D. Freeman. The derivation of direction selectivity in the striate cortex. *Journal of Neuroscience*, 24(14):3583–3591, 2004. ISSN 0270-6474. doi: 10.1523/JNEUROSCI.5398-03.2004. URL https://www.jneurosci.org/content/24/14/3583.

[46] Michael Okun and Ilan Lampl. Instantaneous correlation of excitation and inhibition during ongoing and sensory-evoked activities. *Nature Neuroscience*, 11(5):535–537, May 2008. ISSN 1546-1726. doi: 10.1038/nn.2105. URL https://doi.org/10.1038/nn.2105.

[47] Edward H. Adelson and James R. Bergen. Spatiotemporal energy models for the perception of motion. *J. Opt. Soc. Am. A*, 2(2):284–299, Feb 1985. doi: 10.1364/JOSAA.2.000284. URL http://opg.optica.org/josaa/abstract.cfm?URI=josaa-2-2-284.

[48] Qian Yang, Xianglin Qi, and Wang Yunjiu. Modeling neuronal dynamic coding in primary visual cortex. *Biosystems*, 58(1):203–209, 2000. ISSN 0303-2647. doi: https://doi.org/10.1016/S0303-2647(00)00124-6. URL https://www.sciencedirect.com/science/article/pii/S0303264700001246.

[49] Tony Lindeberg. Generalized gaussian scale-space axiomatics comprising linear scale-space, affine scale-space and spatio-temporal scale-space. *Journal of Mathematical Imaging and Vision*, 40(1): 36–81, May 2011. ISSN 1573-7683. doi: 10.1007/s10851-010-0242-2. URL https://doi.org/10.1007/s10851-010-0242-2.

[50] James M. McFarland, Yuwei Cui, and Daniel A. Butts. Inferring nonlinear neuronal computation based on physiologically plausible inputs. *PLOS Computational Biology*, 9(7):1–18, 07 2013. doi: 10.1371/journal.pcbi.1003143. URL https://doi.org/10.1371/journal.pcbi.1003143.

[51] Milad Hobbi Mobarhan, Geir Halnes, Pablo Martínez-Cañada, Torkel Hafting, Marianne Fyhn, and Gaute T. Einevoll. Firing-rate based network modeling of the dlgn circuit: Effects of cortical feedback on spatiotemporal response properties of relay cells. *PLOS Computational Biology*, 14(5):1–38, 05 2018. doi: 10.1371/journal.pcbi.1006156. URL https://doi.org/10.1371/journal.pcbi.1006156.

[52] S. Dawis, R. Shapley, E. Kaplan, and D. Tranchina. The receptive field organization of x-cells in the cat: Spatiotemporal coupling and asymmetry. *Vision Research*, 24(6):549 – 564, 1984. ISSN 0042-6989. doi: https://doi.org/10.1016/0042-6989(84)90109-3. URL http://www.sciencedirect.com/science/article/pii/0042698984901093.

[53] Wallace B. Thoreson and Stuart C. Mangel. Lateral interactions in the outer retina. *Progress in Retinal and Eye Research*, 31(5):407–441, 2012. ISSN 1350-9462. doi: https://doi.org/10.1016/j.preteyeres.2012.04.003. URL https://www.sciencedirect.com/science/article/pii/S1350946212000286.

[54] Katrin Franke, Philipp Berens, Timm Schubert, Matthias Bethge, Thomas Euler, and Tom Baden. Inhibition decorrelates visual feature representations in the inner retina. *Nature*, 542(7642):439–444, Feb 2017. ISSN 1476-4687. doi: 10.1038/nature21394. URL https://doi.org/10.1038/nature21394.

[55] A. B. Saul and A. L. Humphrey. Evidence of input from lagged cells in the lateral geniculate nucleus to simple cells in cortical area 17 of the cat. *Journal of Neurophysiology*, 68(4):1190–1208, 1992. doi: 10.1152/jn.1992.68.4.1190. URL https://doi.org/10.1152/jn.1992.68.4.1190. PMID: 1432077.

[56] G. C. DeAngelis, I. Ohzawa, and R. D. Freeman. Spatiotemporal organization of simple-cell receptive fields in the cat's striate cortex. ii. linearity of temporal and spatial summation. *Journal of Neurophysiology*, 69(4):1118–1135, 1993. doi: 10.1152/jn.1993.69.4.1118. URL https://doi.org/10.1152/jn.1993.69.4.1118. PMID: 8492152.

[57] D. N. Mastronarde. Two classes of single-input x-cells in cat lateral geniculate nucleus. i. receptive-field properties and classification of cells. *Journal of Neurophysiology*, 57(2):357–380, 1987. doi: 10.1152/jn.1987.57.2.357. URL https://doi.org/10.1152/jn.1987.57.2.357. PMID: 3559684.

[58] Alan B. Saul and Jordan C. Feidler. Development of response timing and direction selectivity in cat visual thalamus and cortex. *Journal of Neuroscience*, 22(7):2945–2955, 2002. ISSN 0270-6474. doi: 10.1523/JNEUROSCI.22-07-02945.2002. URL https://www.jneurosci.org/content/22/7/2945.

[59] R. T. Marrocco. Sustained and transient cells in monkey lateral geniculate nucleus: conduction velocites and response properties. *Journal of Neurophysiology*, 39(2):340–353, 1976. doi: 10.1152/jn.1976.39.2.340. URL https://doi.org/10.1152/jn.1976.39.2.340. PMID: 815516.

[60] Alan B. Saul. Lagged cells in alert monkey lateral geniculate nucleus. *Visual Neuroscience*, 25(5-6):647–659, 2008. doi: 10.1017/S0952523808080784. URL https://doi.org/10.1017/S0952523808080784.

[61] Denise M. Piscopo, Rana N. El-Danaf, Andrew D. Huberman, and Cristopher M. Niell. Diverse visual features encoded in mouse lateral geniculate nucleus. *Journal of Neuroscience*, 33(11):4642–4656, 2013. ISSN 0270-6474. doi: 10.1523/JNEUROSCI.5187-12.2013. URL https://www.jneurosci.org/content/33/11/4642.

[62] Anthony D. Lien and Massimo Scanziani. Cortical direction selectivity emerges at convergence of thalamic synapses. *Nature*, 558(7708):80–86, Jun 2018. ISSN 1476-4687. doi: 10.1038/s41586-018-0148-5. URL https://doi.org/10.1038/s41586-018-0148-5.

[63] Anton Chizhov and Natalia Merkulyeva. Refractory density model of cortical direction selectivity: Lagged-nonlagged, transient-sustained, and on-off thalamic neuron-based mechanisms and intracortical amplification. *PLOS Computational Biology*, 16(10):1–42, 10 2020. doi: 10.1371/journal.pcbi.1008333. URL https://doi.org/10.1371/journal.pcbi.1008333.

[64] B. G. Cleland, M. W. Dubin, and W. R. Levick. Sustained and transient neurones in the cat's retina and lateral geniculate nucleus. *The Journal of Physiology*, 217(2):473–496, 1971. doi: https://doi.org/10.1113/jphysiol.1971.sp009581. URL https://physoc.onlinelibrary.wiley.com/doi/abs/10.1113/jphysiol.1971.sp009581.

[65] Logan Chariker, Robert Shapley, Michael Hawken, and Lai-Sang Young. A theory of direction selectivity for macaque primary visual cortex. *Proceedings of the National Academy of Sciences*, 118(32):e2105062118, 2021. doi: 10.1073/pnas.2105062118. URL https://www.pnas.org/doi/abs/10.1073/pnas.2105062118.

[66] Cyril Monier, Frédéric Chavane, Pierre Baudot, Lyle J Graham, and Yves Frégnac. Orientation and direction selectivity of synaptic inputs in visual cortical neurons: A diversity of combinations produces spike tuning. *Neuron*, 37(4):663 – 680, 2003. ISSN 0896-6273. doi: https://doi.org/

10.1016/S0896-6273(03)00064-3. URL http://www.sciencedirect.com/science/article/pii/S0896627303000643.

[67] L. Federico Rossi, Kenneth D. Harris, and Matteo Carandini. Spatial connectivity matches direction selectivity in visual cortex. *Nature*, 588(7839):648–652, Dec 2020. ISSN 1476-4687. doi: 10.1038/s41586-020-2894-4. URL https://doi.org/10.1038/s41586-020-2894-4.

[68] Margaret S Livingstone. Mechanisms of direction selectivity in macaque v1. *Neuron*, 20(3):509–526, 1998. ISSN 0896-6273. doi: https://doi.org/10.1016/S0896-6273(00)80991-5. URL https://www.sciencedirect.com/science/article/pii/S0896627300809915.